Quasi-Classical Trajectory Calculations of the Thermal Rate Coefficient for the O + OH → O_2 + H Reaction on Realistic Double Many-Body Expansion Potential Energy Surfaces for Ground-State HO_2

L. A. M. Quintales,[†,‡] A. J. C. Varandas,*[,†] and J. M. Alvariño[‡]

Departamento de Química, Universidade de Coimbra, 3049 Coimbra Codex, Portugal, and Departamento de Química Física, Universidad de Salamanca, 37008 Salamanca, Spain *(Received: November 10, 1987)*

Quasi-classical trajectory calculations of the thermal rate coefficient for the title reaction have been carried out over the temperature range $250 \leq T \leq 2500$ K by using two recently reported DMBE potential energy surfaces for the ground state of the hydroperoxyl radical. The results are compared with each other and with experiment. The agreement is good. Our results support previous theoretical calculations by Miller on the Melius–Blint potential energy surface in that nonstatistical "recrossing" effects are very important. For the DMBE II (DMBE III) potential energy surface, these nonstatistical corrections are found to increase from a factor of about 1.2 (1.4) at 250 K to about 2.1 (2.5) at 2500 K. However, they are considerably smaller than the nonstatistical corrections reported by Miller (factors of about 2.2 and 3.3 at the above temperatures). Although due, of course, to topographical differences between the DMBE and Melius–Blint potential energy surfaces, such discrepancy stems also from the different definitions used for HO_2^* complex in the simple chemical model O + OH ⇄ HO_2^* → O_2 + H.

1. Introduction

The O + OH → O_2 + H reaction has been much studied both experimentally[1-4] and theoretically.[5-9] Two major reasons warrant this attention. First, the reverse reaction is the single most important reaction in combustion,[8] being primarily responsible for initiating the chain branching ignition phenomenon in the oxidation of molecular hydrogen and most hydrocarbon fuels.[10] Second, the title reaction is a good prototype neutral–neutral reaction occurring on a single adiabatic potential energy surface that has no potential barrier and proceeds over a relatively deep potential. Additional motivations come from the importance of the O + OH long-range forces on the dynamics of the title reaction[7,9] and from the availability of extensive experimental work that makes the corresponding thermal rate coefficient known with reliability over a wide range of temperatures.

Most dynamics calculations of the title and reverse reactions have used the Melius–Blint[11] functional form for the ground-state potential energy surface of HO_2. Of them, the quasi-classical trajectory method has been used to calculate thermal rate coefficients for the title and reverse reactions,[5,8] some dynamical attributes of the H + O_2 → OH + O reaction,[12,13] and the dynamics of the HO_2 dissociation.[14] Rai and Truhlar[6] used variational transition-state theory on the Melius–Blint potential energy surface to calculate the thermal rate coefficient of the title reaction as a function of temperature.

Other 3D functional forms used for dynamics studies include the LEPS function of Gauss[15] and the many-body expansion[16] (MBE) potential energy surface of Murrell et al.,[17] both of which have been used for quasi-classical trajectory calculations[15,18] of the thermal rate coefficient of the title and reverse reactions. Simpler potential models have been used to study the title and reverse reactions within the adiabatic channel model.[2,9] Clary[7] has combined approximate quantum scattering calculations with long-range potentials to calculate the rate constant for the title reaction. Most recently, Lemon and Hase[19] reported trajectory calculations for highly excited HO_2 on an analytic surface constructed from switching functions and extensions of the BEBO[20] concepts. Note that this surface is written in terms of two bond-distances (referring to OH and OO) and one angle (HOO) and hence cannot describe H-atom migration between the oxygen atoms.

Recently,[21] we suggested a new analytic potential energy surface for ground-state HO_2 based on the double many-body expansion (DMBE)[22-24] method. Through this method it has been possible to combine a good description of the valence region of the potential surface (which conforms with the three-body energy contributions from the Melius–Blint ab initio electronic structure calculations) with the appropriate asymptotic long-range forces. Our immediate goal was therefore to use that potential for dynamics studies of the title and reverse reactions. Despite some improvement over previous forms for the HO_2 potential energy surface, it turned out from preliminary trajectory studies that the thermal rate coefficients for the title reaction were in poor agreement with experiment. Most recently, this problem has been identified, and two new DMBE potential surfaces were proposed[25] for H_2O-($\tilde{X}^2A''$). They have been denoted DMBE II and DMBE III in the original paper, and we keep the same notation in the current work. Thus, it is our purpose in this paper to show that both these DMBE potentials produce thermal rate coefficients for the title reaction in good agreement with the best available experimental values.

The structure of this paper is as follows. In section 2, we make

[†] Universidade de Coimbra.
[‡] Universidad de Salamanca.

(1) Howard, M. J.; Smith I. W. *J. Chem. Soc., Faraday Trans. 2* **1981**, *77*, 997.
(2) Cobos, C. J.; Hipler, H.; Troe, J. *J. Phys. Chem.* **1985**, *89*, 342.
(3) For a critical evaluation of the experimental data see: Cohen, N.; Westberg, K. R. *J. Phys. Chem. Ref. Data* **1983**, *12*, 531.
(4) Frank, P.; Just, Th. *Ber. Bunsen-Ges. Phys. Chem.* **1985**, *89*, 181.
(5) Miller, J. A. *J. Chem. Phys.* **1981**, *74*, 5120. Miller, J. A. *J. Chem. Phys.* **1981**, *75*, 5349.
(6) Rai, S. N.; Truhlar, D. G. *J. Chem. Phys.* **1983**, *79*, 6046.
(7) (a) Clary, D. C.; Werner, H. J. *Chem. Phys. Lett.* **1984**, *112*, 346. (b) Clary, D. C. *Mol. Phys.* **1984**, *53*, 3.
(8) Miller, J. A. *J. Chem. Phys.* **1986**, *84*, 6170.
(9) Troe, J. *J. Phys. Chem.* **1986**, *90*, 3485.
(10) Benson, S. W.; Nangia, P. S. *Acc. Chem. Res.* **1979**, *12*, 223.
(11) Melius, C. F.; Blint, R. J. *Chem. Phys. Lett.* **1979**, *64*, 183.
(12) Bottemley, M.; Bradley, J. N.; Gilbert, J. R. *Int. J. Chem. Kinet.* **1981**, *13*, 957.
(13) Kleinermans, K.; Schinke, R. *J. Chem. Phys.* **1984**, *80*, 1440.
(14) Miller, J. A.; Brown, N. J. *J. Chem. Phys.* **1982**, *86*, 772.
(15) Gauss, A., Jr. *J. Chem. Phys.* **1978**, *68*, 1689.
(16) Murrell, J. N.; Carter, S.; Farantos, S. C.; Huxley, P.; Varandas, A. J. C. *Molecular Potential Energy Functions*; Wiley: Chichester, 1984.
(17) Farantos, S. C.; Leisegang, E.; Murrell, J. N.; Sorbie, K. S.; Teixeira Dias, J. J. C.; Varandas, A. J. C. *Mol. Phys.* **1977**, *34*, 947.
(18) Mann, A. P. C., unpublished work quoted in ref 50 of ref 7b.
(19) Lemon, W. J.; Hase, W. *J. Phys. Chem.* **1987**, *91*, 1596.
(20) Johnson, H. S. *Gas Phase Reaction Rate Theory*; Ronald: New York, 1966; p 55.
(21) Varandas, A. J. C.; Brandão, J. *Mol. Phys.* **1986**, *57*, 387.
(22) Varandas, A. J. C. *THEOCHEM* **1985**, *120*, 401.
(23) Varandas, A. J. C. In *Structure and Dynamics of Weakly Bound Complexes*; Weber, A., Ed.; D. Reidel: Dordrecht, 1987; p 357.
(24) Varandas, A. J. C. *Adv. Chem. Phys.*, in press.
(25) Varandas, A. J. C.; Brandão, J.; Quintales, L. A. M. *J. Phys. Chem.* **1988**, *92*, 3732.

0022-3654/88/2092-4552$01.50/0

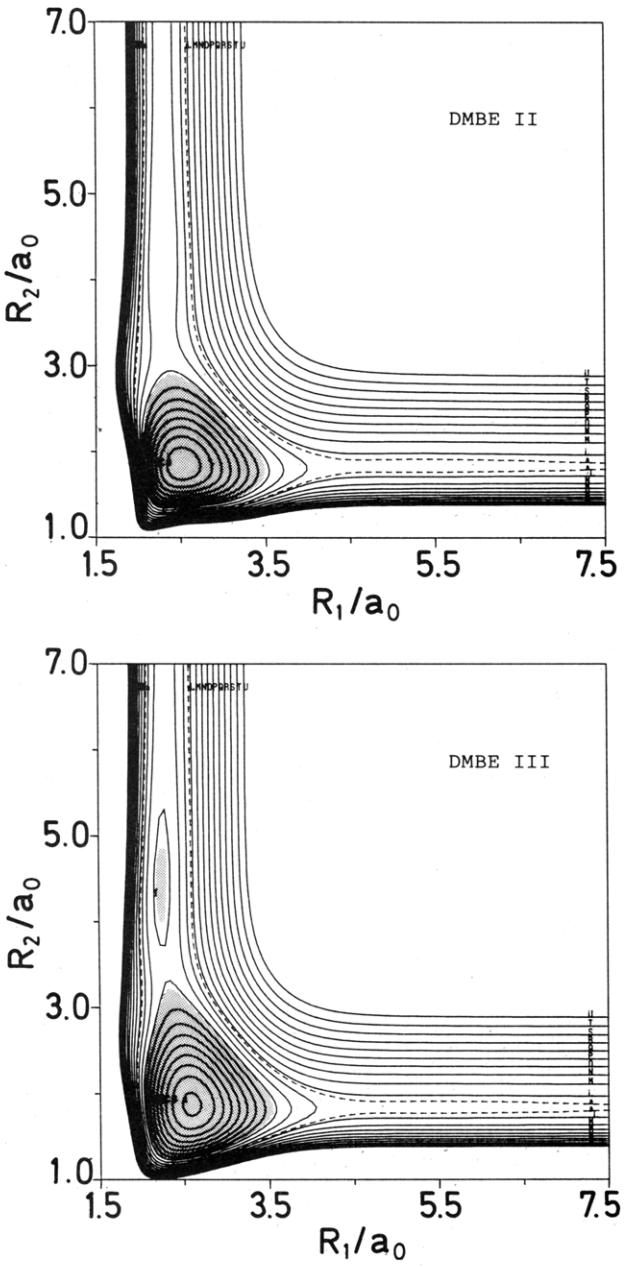

Figure 1. Contour plots for the stretching of the OO and OH bonds in $HO_2(\tilde{X}^2A'')$ with the HOO angle fixed at the equilibrium value. The upper plot refers to the DMBE II potential energy surface while the other is for the DMBE III potential surface. Contours are equally spaced by $0.01E_h$, starting at $A = -0.277E_h$. The dashed line (contour a) indicates the energy contour corresponding to the O + OH dissociation limit, while the shaded area represents the regions of configuration space for which the energy lies 0.2 eV below the H + O_2 dissociation limit.

a brief assessment of the most relevant topographical features of the DMBE II and DMBE III potential energy surfaces. The methodology and mathematical forms used in the quasi-classical trajectory calculations are described in section 3. The results and their discussion are presented in section 4. Section 5 summarizes the conclusions.

2. HO_2 DMBE Potential Energy Surfaces

The potential surfaces used for the current trajectory calculations have been described in detail in ref 25, and hence only the important features for this work are surveyed here. Figure 1 shows bond-stretching contour plots of the OO and OH distances (R_1 and R_2 or R_3, respectively) for the OOH angle fixed at the equilibrium value. In Figure 2 we show similar contours but for an O atom moving around a OH diatomic the bond length of which is partially optimized (hartree (E_h) = au of energy =

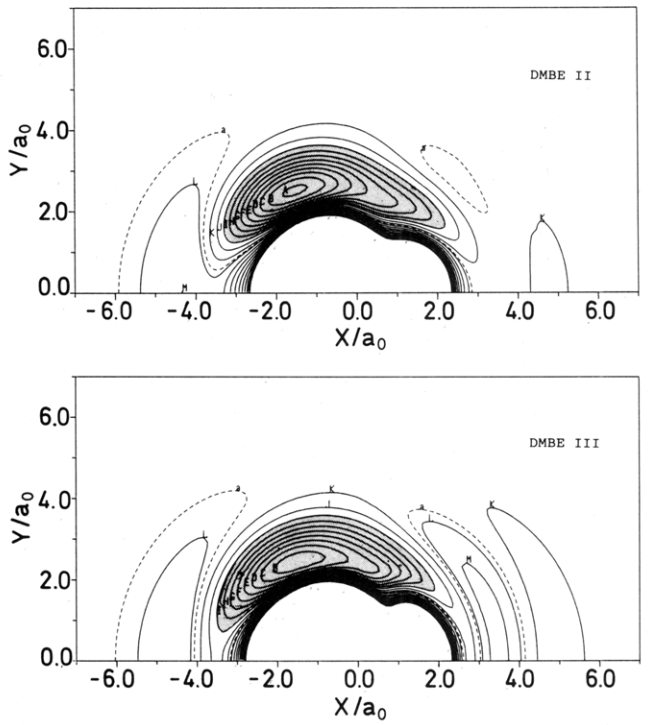

Figure 2. Contour plots for an O atom moving around an OH diatomic the bond length of which is partially relaxed ($1.63 \leq R_2 \leq 2.23\ a_0$) at each position of the O atom so as to give the lowest potential energy. Contours and shaded area are as in Figure 1.

27.211 652 eV = 4.359 821 5 aJ; bohr (a_0) = au of length = 0.529 177 Å = 0.052 917 7 nm; $1.63 \leq R_2 \leq 2.23\ a_0$) at each position of the remaining O atom. Shown by the dashed lines in Figures 1 and 2 is the energy corresponding to the O + OH dissociation limit, while the shaded area delimits the region of configuration space lying 0.2 eV below the H + O_2 dissociation limit. The notable feature is the absence of an energy barrier at both the O + OH and H + O_2 asymptotic channels. We also observe the hydrogen-bonded minimum occurring for collinear OHO geometries, which is found to control the early dynamical stages of O attack to OH. The reader is referred to ref 25 and 26 for further graphical representations of the DMBE II and DMBE III potential surfaces used in the present calculations.

3. Computational Methods

The quasi-classical trajectory method as applied to atom–diatom collisions has been used to calculate total reactive cross sections $\sigma^r(T)$ for thermalized reactants as a function of temperature. The method is well documented in the literature,[27] and hence no details will be given here. According to this method

$$\sigma^r(T) = \pi b_{max}^2 N^r/N \tag{1}$$

where b_{max} is the maximum impact parameter that leads to reaction, and N^r/N is the fraction of trajectories that are reactive. The 68% confidence intervals are similarly given by

$$\Delta\sigma^r(T) = [(N - N^r)/NN^r]^{1/2}\sigma^r(T) \tag{2}$$

The thermal rate coefficient can be calculated from $\sigma^r(T)$ by the expression

$$k(T) = \bar{v}\sigma^r(T)\, f(T) \tag{3}$$

where $\bar{v} = (8k_BT/\pi\mu_{O,OH})^{1/2}$, and

$$f(T) = 2\{[5 + 3\exp(-228/T) + \exp(-326/T)] \times [2 + 2\exp(-205/T)]\}^{-1} \tag{4}$$

(26) Varandas, A. J. C. *Chem. Phys. Lett.* **1987**, *138*, 455.
(27) Truhlar, D. G.; Muckerman, J. T. In *Atom–Molecule Collision Theory*; Bernstein, R. B., Ed.; Plenum: New York, 1981; p 475.

TABLE I: Summary of the Trajectory Calculations

T/K	b_{max}/Å	N	N^r_{OO}	N^r_{OH}	N^r_{tot}
		DMBE II			
250	7.0	491	156	36	192
500	6.0	491	148	29	177
1000	6.0	498	83	32	115
1500	6.0	500	67	33	100
2000	6.0	500	50	30	80
2500	5.0	411	52	54	106
		DMBE III			
250	7.0	480	130	8	138
500	7.0	667	123	8	131
750	7.0	494	71	5	76
1000	6.0	499	73	16	89
1250	6.5	992	114	19	133
1500	6.0	498	53	7	60
1750	6.0	496	52	18	70
2000	6.0	499	45	17	62
2250	5.5	497	52	18	70
2500	5.0	499	59	26	85

TABLE II: Numerical Values of Least-Squares Parameters in Eq 6

parameter	ref 3	DMBE II	DMBE III
A/(dm^3 mol^{-1} s^{-1} K^{-m})	4.5 (+11)	3.04 (+11)	1.07 (+11)
m	−0.5 (0)	−0.45 (0)	−0.33 (0)
E/(J mol^{-1})	−30	−46.3	−480

is a statistical weight factor accounting for the electronic degeneracies;[7] all other symbols have their usual meaning.

4. Results and Discussion

A total of about 8500 quasi-classical trajectories have been run on the DMBE II and DMBE III potential energy surfaces that were distributed over 10 temperatures in the range $250 \leq T \leq 2500$ K, as compiled in Table I. In this table, N^r_{OO} is the number of reactive trajectories leading to the exoergic reaction

$$O + OH \rightarrow O_2 + H \qquad (a)$$

N^r_{OH} denotes those that originated H-atom exchange between the two O atoms:

$$O_a + O_bH \rightarrow O_aH + O_b \qquad (b)$$

and N^r_{tot} represents the total number of reactive trajectories, $N^r_{tot} = N^r_{OO} + N^r_{OH}$. We note that many O + OH trajectories turn out to be of the long-lived type, which makes their integration computationally very expensive (the time duration per trajectory is typically 8–30 min in the dedicated Data General DS 7540 computer available at the Theoretical Chemistry Group in the University of Coimbra). This fact prevented us from carrying out a more extensive calculation. However, the data compiled in Table I are sufficient to give an error limit of about ±10% for reaction a. Of course, much poorer statistics will be obtained for reaction b due to the smaller number of reactive events for this channel and to the fact that b_{max} has been optimized for reaction a. Nevertheless, the results for reaction b are still presented in Table I for the sake of completeness.

Figure 3 reports the computed thermal rate coefficients as a function of temperature together with the associated error bars. Also shown for comparison are the experimental correlation of Cohen and Westberg[3] and the latest experimental estimates of Frank and Just,[4] which have indirectly been obtained by using the equilibrium constant for the process $H + O_2 \rightleftarrows OH + O$ and the rate coefficient for the $H + O_2 \rightarrow OH + O$ reaction. Since these two sources encompass most of the experimental data reported in the literature, we deemed unnecessary any further comparisons with experiment. Note that the dotted lines in Figure 3 account for the uncertainty associated with the Cohen–Westberg correlation (this is shown by the dash–dot line) and the Frank–Just results (dashed line), while the heavy lines represent the best least-squares fits of our data to the form

$$k(T) = AT^m \exp(-E/RT) \qquad (5)$$

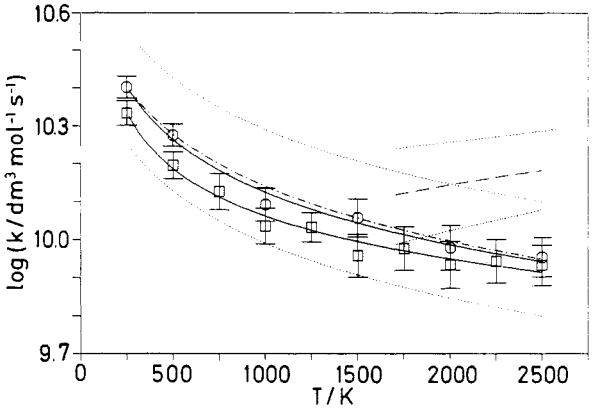

Figure 3. Plot of log ($k(T)$) against T for the reaction $O + OH \rightarrow O_2 + H$. Shown in this plot are the current results for the DMBE II and DMBE III potential energy surfaces, the experimental correlation of Cohen and Westberg[3] (–·–) and the experimental results of Frank and Just[4] (– – –). The dotted lines represent the uncertainty of the experimental data, while that of the theoretical data is indicated by the error bars. The lines through the theoretical points represent the best least-squares fits based on eq 5.

where A, m, and E are the least-squares variables. Table II summarizes the numerical values obtained from our fitting procedure. Note that no physical meaning can be attributed to A and E although eq 5 has been written in the form of an Arrhenius-type expression. The results may nevertheless allow a comparison with those presented by Cohen and Westberg, who used the same analytic form but with m fixed at $m = -0.5$. (As expected from the data of Table I, the thermal rate coefficients for the isoergic H-atom exchange process were found to decrease somewhat with increasing temperature at the lower temperatures studied, followed by an increasing T dependence at the higher temperatures. However, due to their poor statistics, such results are omitted.) It is gratifying to note that the theoretical values of $k(T)$ for the title reaction fall, for both the DMBE II and DMBE III potential energy surfaces, within the error limits of the experimental Cohen–Westberg correlation, although they lie somewhat below the more recent estimates of Frank and Just[4] for the high-temperature regime. However, our results disagree with those of Frank and Just in that they do not predict a positive though small activation energy over the range $1700 \leq T \leq 2500$ K. Finally, we observe that the thermal rate coefficients calculated from the HO_2 DMBE I potential energy surface of Ref 21 considerably underestimate the experimental results. This failure is attributed to a small barrier appearing in the O + OH entrance channel of the HO_2 DMBE I potential energy surface.

We now address the question raised by Miller[8] concerning the so-called recrossing phenomenon. To answer this problem, we follow Miller and think of the title reaction in terms of the simple chemical model

$$O + OH \rightleftarrows HO_2^* \rightarrow O_2 + H \qquad (c)$$

where the complex is denoted HO_2^*. To distinguish between trajectories that form or do not form this complex, Miller plotted histograms of the minimum O–O separation. He observed that these O–O distributions were bimodal at both 500 and 2500 K. The trajectories in the inner grouping of bins were those that penetrated past a critical O–O separation (which was taken as the O–O distance in equilibrium HO_2, i.e., $R^0_{OO} = 1.36$ Å) and were said to have formed the HO_2^* complex. Those in the outer grouping of bins correspond to those rejected before reaching an O–O separation equal to R^0_{OO} and were considered as having not formed an HO_2^* complex. For example, at 500 K, Miller found that the reaction probability to form $O_2 + H$ was 15.8%, whereas the probability of forming complexes was 39%. These percentages change, at 2500 K, to 6.5% and 21%, in the above order. Thus, a large fraction of complexes were found not forming products.

TABLE III: Nonstatistical Recrossing Ratios, P_r/P_c, for the O + OH → O_2 + H Reaction on the DMBE II and DMBE III Potential Energy Surfaces[a]

T/K	DMBE II	DMBE III	T/K	DMBE II	DMBE III
250	0.708	0.823	1500	0.528	0.679
500	0.713	0.794	1750		0.565
750		0.755	2000	0.446	0.542
1000	0.569	0.608	2250		0.500
1250		0.663	2500	0.414	0.472

[a] P_r is the probability of forming H + O_2 and P_c the probability of HO_2* complex formation; see also the text.

As is well-known, RRKM (or statistical) theories[2,5] rely on the assumption that essentially all HO_2* complexes formed should decompose into H + O_2. In fact, conventional statistical models of $k(T)$ for the title reaction have been shown to reduce to the transition-state theory rate coefficient for HO_2* complex formation, particularly at low temperature.[5] In contrast, Miller[8] has found that only 40% of those complexes formed products at 500 K and only 30% formed them at 2500 K. As a result, he remarked that theories (statistical or dynamical) that take into account only the O + OH reaction channel of the potential are to be viewed with suspicion.[2,7,9] Within this spirit he suggested that the variational transition-state theory calculations of Rai and Truhlar[6] should be corrected by a temperature-dependent factor, making such correction larger at higher temperatures. In this way he has been able to bridge the gap between theory and experiment originally reported by Rai and Truhlar.

Miller's definition[8] of nonstatistical recrossing differs, however, in a subtle way from ordinary statistical recrossing where the trajectory once crossing the so-called transition-state dividing surface (TSDS) does not recross back to reactants. In fact, the term nonstatistical is used by Miller to describe trajectories having one or more O–O inner turning points (and hence considered to have formed a HO_2* complex) which redissociate into O + OH. Of course, statistical theories predict some recrossing at high temperatures, but for the present reaction it may be considered a minor effect at low and moderate temperatures. Note that the ratio of the probability of dissociating into O + OH to the probability of dissociation into H + O_2 is of the order of $\exp(-\Delta E_{TS}/RT)$ where ΔE_{TS} is the difference in potential energy (including the zero-point vibrational energy) of the appropriate transition states. Miller's definition of nonstatistical recrossing is therefore consistent with the assumption adopted in statistical theories that once an appropriate TSDS is crossed by a trajectory, a complex is formed, although it is unable to distinguish between statistical and nonstatistical recrossing.

Since the statistical definition of recrossing cannot be easily implemented into the trajectory program, this prompted us to use another definition of the HO_2* complex that affords a simple, yet meaningful, picture. We define HO_2* complex as a species whose energy is at least ΔE = 0.2 eV below that of the H + O_2 products channel. This definition is corroborated from an eye analysis of the traditional bond distances against time plots, where the complex lifetime corresponds to the time interval for which the lines representing the three bond distances are mixed up and these distances are similar in magnitude. Thus, we have selected ΔE from the requirement that the complex lifetime measured by the time the trajectory remains below that limiting energy should be similar to that obtained in the above traditional way. The regions of configuration space associated to such HO_2* complexes are shown in Figures 1 and 2 by the shaded areas. We have therefore calculated the percentage of trajectories that entered one or more times those shaded regions (i.e., formed HO_2* complexes) but did not form H + O_2 products. Note that, like Miller's,[8] the current definition of the HO_2* complex is consistent with the assumption adopted in statistical theories although it is unable to distinguish statistical and nonstatistical recrossing. Our use of the latter term stems therefore from the energetic reasons presented above, which leave us to expect the present definition of HO_2* complex to provide a reliable estimate of the nonstatistical recrossing. Note further that no attempt has been made to discard those trajectories that recrossed back to reactants with an energy less than the zero-point energy of OH (these are, of course, unphysical and have no meaning in transition-state theory) as these should not affect the general trends of our observations. Thus, the ratios reported in the current work represent an upper bound of the true nonstatistical recrossing ratios for the adopted definition of HO_2* complex.

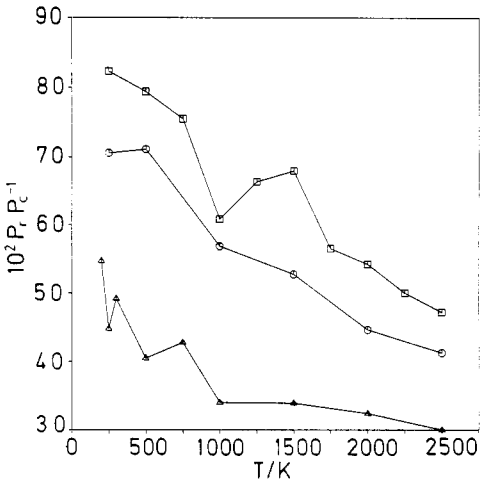

Figure 4. Nonstatistical corrections to $k(T)$ against T, O + OH ⇄ HO_2* → H + O_2. P_r is the probability of forming H + O_2, and P_c the probability of complex formation. The HO_2* complexes were defined by monitoring the potential energy along the trajectory and said to have been formed when the trajectory enters the region 0.2 eV below the H + O_2 asymptotic channel. Key for symbols: △, Miller;[8] ○, this work, DMBE II; □, this work, DMBE III.

Table III summarizes the nonstatistical recrossing ratios obtained in the present work for both the DMBE II and DMBE III potential energy surfaces while Figure 4 compares them with the results reported by Miller[8] for the Melius–Blint potential energy surface. (Of course, a more rigorous comparison would require the use of a common potential energy surface to compare both definitions of HO_2* complex. Although we have not carried out such a comparison in the present work, we note that the reported discrepancies in the nonstatistical corrections are too large to afford an explanation only with a basis on the topographical differences between the DMBE and the Melius–Blint potential energy surfaces.) Two salient features are apparent from Figure 4. First, we find a substantially smaller (and probably physically more reasonable) rate for nonstatistical recrossing based on the current definition of HO_2* complex. Second, we agree with Miller that although smaller than he reported, nonstatistical recrossing effects are far from being negligible. Finally, and also in agreement with Miller, our results show an increasing percentage of such recrossing with increasing temperature. Thus, we support his remarks that theories (dynamical or statistical) that neglect nonstatistical recrossing effects for the title reaction should be viewed with caution.

5. Conclusions

We have shown that the HO_2 DMBE potential energy surfaces reported in ref 25 predict thermal rate coefficients in good agreement with experiment. Since in addition the DMBE III potential reproduces the experimental spectroscopic force field of the hydroperoxyl radical, we are led to believe that it is, overall, the most realistic representation currently available for the potential energy surface of ground-state HO_2.

Acknowledgment. Financial support from the Instituto Nacional de Investigação Científica (INIC), Lisbon, Portugal, is gratefully acknowledged. This project has also benefited from a Portuguese–Spanish joint venture ("Acção Integrada"). L. A.M.Q. thanks the Ministerio de Educacion y Ciencia, Spain, for an FPI grant and the University of Salamanca for leave of absence.

Registry No. O, 17778-80-2; OH, 3352-57-6.